2554 *Macromolecules* **2010**, *43*, 2554–2563
DOI: 10.1021/ma901937r

Macromolecules
ARTICLE

Large Strain and Fracture Properties of Poly(dimethylacrylamide)/Silica Hybrid Hydrogels

Wei-Chun Lin, Wei Fan, Alba Marcellan, Dominique Hourdet, and Costantino Creton*

Laboratoire Physico-Chimie des Polymères et des Milieux Dispersés (PPMD), ESPCI 10 rue Vauquelin, 75231 Paris, Cedex 05, France

Received September 1, 2009; Revised Manuscript Received January 22, 2010

ABSTRACT: The synthesis and mechanical characterization of novel, tough poly(*N*,*N*-dimethylacrylamide) (PDMA)−silica hydrogel hybrids are presented to understand the role played by strong physical interactions between silica nanoparticles and the PDMA polymer on the properties of chemically cross-linked highly swollen PDMA networks. A detailed comparison of the hybrids with unmodified PDMA gels indicates that the incorporation of silica nanoparticles in the hydrogel increases the compression strength and the fracture toughness of notched samples up to an order of magnitude while increasing its modulus by a factor of 6 with a volume fraction of particles of the order of only 7%. The hybrid gels present a strain-dependent hysteresis but no permanent damage or residual strain upon unloading even after repeated cycling, a very unique property for such tough hydrogels. The reason for this exceptional increase in toughness is attributed mainly to the combined effect of breakable silica/polymer bonds and of a wide distribution of elastic chain lengths.

Introduction

The idea of a tough hydrogel was once a paradox. In the past, this class of soft materials was often regarded as weak and fragile due to their highly swollen structure. However, recent demand for tough polymer materials in biomedical applications has led to the development of robust hydrogels.[1] Such improvements in the strength of these gels has thereby generated interest in the understanding of high strain deformation and fracture mechanics, as well as toughening mechanisms, in general hydrogel systems.

To date, the most important practical advances have primarily been limited to physical gels and complex cross-linked systems. For example, recent progress on physical gels has led to materials with very high extensibilities[2] while developments on double network gels, which result from the synthesis of a highly cross-linked network with a loosely entangled one, have produced high modulus systems with large compressive fracture toughnesses and compressive strengths.[1] The understanding of what makes such gels hard to break is important in that they pave the way for exploring and improving simple covalent cross-linked systems, an avenue of research that has been thus far neglected.

The attention to physical gels in recent years has been catalyzed by the adaptation of techniques traditionally used for rubbers, by the study of the fracture properties of these systems,[3,4] and by the discovery of an important enhancement of their mechanical performance through inorganic fillers to their structures.[2,5,6] Fracture experiments on gelatin and triblock copolymers clearly demonstrate that the fracture toughness, G_c, and sometimes the fracture mechanisms of some physical gels are notably crack speed dependent. This behavior suggests the existence of rate-dependent dissipative mechanisms at the crack tip. The energy release rate of gelatin varies linearly with crack velocity,[3] while a power law describes the fracture behavior of triblock gels.[4] The rate sensitivity of gelatin also increases with the amount of cross-linking.[3] Fracture energies for these physical gels have been observed to be on the order of ∼2−100 J/m^2 for gelatin[3] and ∼10−100 J/m^2 for the acrylic triblock gels.[4] While these values of fracture energy are much lower when compared to those reported for rubbers,[7] they are significantly higher than what is typically observed for chemically cross-linked hydrogels[8] where a crack speed dependence is rarely observed.

The observed enhancements in the mechanical performance of complex gels have therefore renewed interest in these materials. The introduction of clay sheets during the synthesis of poly(*N*,*N*-dimethylacrylamide) (PDMA) gels without a chemical cross-linking agent has led to physical nanocomposite hydrogels that exhibit high transparency and large elongations near to or greater than 1500%.[5] These materials demonstrate decreased swelling ratios with increased concentrations of clay and polymer, suggesting that the clay sheets function as high functionality cross-link points.[5] Such high functionality cross-link points are thought to be essential for the high strength of the material: Under large scale deformation, when one chain fails, the even redistribution of load to other chains is possible, avoiding severe stress concentrations.[9] This strategy has been applied and extensively studied for other physical polymer−clay systems, such as those made from poly(*N*-isopropylacrylamide) (PNIPAM),[6,10] poly(*N*,*N*-dimethylacrylamide) (PDMA),[5] and polyacrylamide (PAAm).[11] Although this explanation is reasonable for the observed behavior of such gels, it is not a sufficient one since several inorganic fillers have been tried and only a few actually work well;[12] the underlying reason for the high toughness of these gels has yet to be fully understood.

Through the manipulation of architecture, the toughening of hydrogels has extended to the use of chemically cross-linked interpenetrated networks. Robust gels are created when a highly cross-linked network is synthesized as an interpenetrated network with a second more loosely cross-linked one.[13] The toughest of these so-called chemically cross-linked double network gels can withstand compressive pressures on the order of tens of MPa.[13]

*Corresponding author. E-mail: costantino.creton@espci.fr.

 Published on Web 02/04/2010

Their fracture energies are on the order of hundreds of J/m^2 [13] and are weakly dependent on crack speed.[14] Under large strain deformation and presumably at the crack tip during fracture, the key strengthening mechanism of these materials has been proposed to be from both a high degree of heterogeneity in their first network[15] and energy dissipation due to the delocalized fracture of the bonds of the first network in a large volume around the crack tip.[16,17]

Recent post-mortem optical observations of the damaged region near the crack tip have confirmed this interpretation.[18] Although these gels exhibit high toughness, irreversible bond breakage occurs during deformation. After the first cycle of loading−unloading, the gels show a permanent reduction in stiffness and energy dissipation. This permanent change in mechanical properties is one potential drawback of these gels if they are to be used in applications where cyclic loading is present and mechanical reproducibility is required. Furthermore, their synthesis in two steps by UV cross-linking is rather complex, sensitive to exact UV irradiation conditions, and the necessity to swell to equilibrium makes it more difficult to control the final geometry of the gel sample.

The properties of mechanically robust physical gels and complex cross-linked gels indicate that their polymer network structure plays an important role in strengthening and toughening these materials. On the basis of this idea, we present and characterize in this paper a novel chemically cross-linked polymer hydrogel hybrid that is formed from polymerizing and slightly cross-linking *N,N*-dimethylacrylamide (DMA) in the presence of silica nanoparticles. The reason for using silica as a filler stems from previous results obtained with fully un-cross-linked PDMA chains. Petit et al. have shown that the adsorption of PDMA chains on silica nanoparticles leads to the formation of a physical network,[19] implying that the strength of the adsorption will be important for the mechanical properties even in the case where both physical adsorption and chemical covalent bonds are present. Such chemically cross-linked gels containing physically adsorbed polymers on silica nanoparticles materials provide a very general route for improving the properties of hydrogels. This type of architecture is widely used for filled rubbers where the chemically cross-linked rubber structure coexists with a physically interacting network of filler particles.[20]

In this work, we first present the synthesis of the gels. The structural and mechanical characterization of the gels follows, where viscoelastic properties, small and large strain compression measurements, hysteresis in compression, and fracture toughness of notched samples are considered. Results are then discussed, and a general model of toughening for filled gels is proposed.

Experiment

Gel Preparation. *Materials*. A series of PDMA−silica hybrids and a conventional, pure chemically cross-linked PDMA gel were concurrently made. The reactants used to synthesize the chemical network PDMA−silica hydrogel hybrids were the same as those used to form the pure chemically cross-linked PDMA gels. Formulation of the pure chemical PDMA required *N,N*-dimethylacrylamide (DMA) (Aldrich, 99%) monomer, *N*, *N*-methylenebis(acrylamide) (MBA) (Fluka, 99%) cross-linker, tetramethylethylenediamine (TEMED) (Aldrich, 99%), and $K_2S_2O_8$ (KPS) (Prolabo, 99%) as redox initiator. These materials were used as received without further purification. The addition of Milli-Q ultrapure water was used during synthesis as well as for swelling in all the systems.

For the hybrid systems, silica nanoparticles were added during the synthesis. Silica nanoparticles in a water suspension (Ludox SM30) were kindly provided by IMCD (France). They were used as received without any modification. Measurements from dynamic light scattering give a mean radius R of 9.3 nm with a standard deviation of 0.5 nm and a specific surface δ of 140 m^2/g. The measurement of the specific surface assumes that the density ρ is 2.3 g/cm^3 and can be calculated from $\delta = 3/\rho R$.

Table 1. Volume Fraction, ϕ, of the Silica and DMA Values Used in the Synthesis of the Hybrids (Preparation Conditions) and during Testing (Swelled to Equilibrium) Conditions[a]

nomenclature	preparation conditions		testing conditions in deionized water	
si(ϕ_{silica}:ϕ_{DMA}) × 100	ϕ_{silica}	ϕ_{DMA}	ϕ_{silica}	ϕ_{DMA}
si0	0	0.11	0	0.062
si25	0.030	0.11	$(0.015 \pm 1.1) \times 10^{-3}$	0.051
si50	0.059	0.11	$(0.034 \pm 3.8) \times 10^{-4}$	0.061
si75	0.086	0.11	$(0.054 \pm 3.7) \times 10^{-4}$	0.064
si100	0.13	0.12	$(0.067 \pm 3.1) \times 10^{-3}$	0.059

[a] The nomenclature for each sample is based on the ratio of silica to DMA volume fraction and provided in the table.

Polymer Gel Synthesis. Standard techniques were used to synthesize the PDMA gels and applied to the formation of the hybrids. Fixed molar ratios of [DMA]:[MBA] at 100:1, i.e., theoretically one cross-link point per 100 monomers, and [DMA]:[KPS]:[TEMED] at 100:1:1 were used for all the gels. The amount of silica and water varied in each sample. Table 1 shows the volume fraction of silica and monomer in the hydrogels made at initial synthesis conditions and during testing conditions at swelling equilibrium. The nomenclature of each sample is noted in the first column of Table 1 and based on the volume fraction ratio of silica to DMA multiplied by 100. The density of dry DMA used in these systems is 0.962 g/mL.

The amount of silica present in each hybrid after swelling was reverified using thermogravimetric analysis (TGA) experiments on swollen samples. In the TGA, each swollen sample was heated to 100 °C at a rate of 10 °C/min and held for 30 min. After this initial heating cycle, the sample was heated to 1000 °C at a rate of 10 °C/min to ensure removal of all excess organic material. Polymer ashes were considered negligible. The amount of silica found by TGA always was either identical to the theoretical value or slightly superior, clearly demonstrating that the silica nanoparticles did not escape in the free water during the swelling to equilibrium stage. No residual monomer was detected by GPC after extraction, and the sol fraction was not measurable for the pure PDMA and for the silica filled samples.

To form the gel network at room temperature, a solution of DMA and MBA was prepared and mixed for 30 min. KPS was then added, and the solution was bubbled under nitrogen and stirred for 15 min. Appropriate amounts of Si nanoparticles and/or water were added into the DMA solution and bubbled under nitrogen for another 30 min. The total monomer volume fraction was kept around 11% for all gels at the preparation conditions and can be seen from Table 1.

The solutions were then moved into a nitrogen atmosphere, where 45 μL of TEMED co-initiator was added. Each solution was then cast into prepared silanized glass molds to form flat layers, and the samples were left for 24 h under a nitrogen atmosphere to ensure complete gelation. After demolding, the gels underwent a solvent exchange for 3 days to remove excess residual byproduct and were swollen to equilibrium in water. The volume fraction of polymer in the testing conditions varied then between 5.1 and 6.4%, as shown in Table 1.

The gels were stored in a water environment at room temperature. Samples of the appropriate dimensions for mechanical testing were cut from the flat layers.

Preparation of Glass Molds. Molds for the gels were made from placing spacers with a height from 1 to 4 mm between silanized, flat glass plates. Because PDMA is quite adhesive to glass, hydrophobic modification of glass plates was necessary. Each glass plate was decontaminated and then plasma-treated to prepare for the silanization process. To minimize surface impurities, the glass substrates were first immersed into a

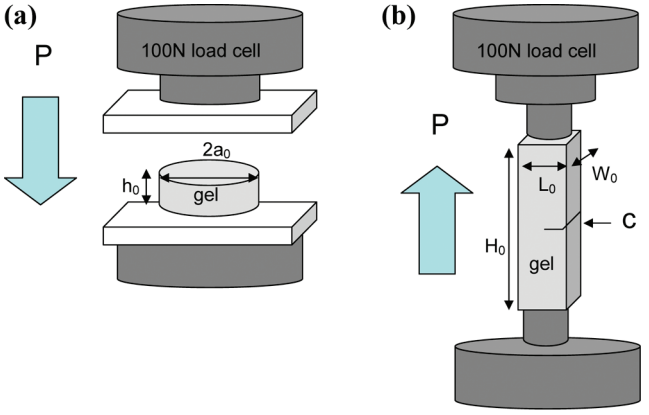

Figure 1. Schematic of (a) compression and (b) single edge notch (SEN) tests.

solution of 5% hydrochloric acid for 4 h under ultrasonication. The plates were rinsed and agitated with deionized, distilled water for 15 min. A second rinsing in water was performed, followed by plasma treatment for 15 min. Immediately after plasma treatment, the glass plates were submersed and gently agitated in a mixture of 5% octadecyltrichlorosilane (OTS, Gelest) in toluene for 1−2 min. Excess material on the surfaces was rinsed off with toluene for 2−3 min. The resulting silane layer was cured at 110 °C for 20 min.

Analytical Methods. *Swelling Experiments*. Swelling experiments were performed on the gels. One sample was cut from each gel without the addition of water after gelation and weighed as-prepared. The sample was then swelled to equilibrium in pure water or in a 1 M NaCl solution, and the swollen weight of the gel was recorded over 4 days to ensure that the gels were at equilibrium. The amount of dry polymer was estimated from the amount of monomer, assuming 100% conversion.

Dynamic Mechanical Analysis. Oscillating compression tests were performed on the hydrogels at 25 °C with a TA Q800 dynamic mechanical analyzer. Cylindrical disks with a radius, a, of 4 mm and an initial thickness, h_0, of 6 mm were cut from the molded gel layers and swollen in deionized water prior to the tests. The disks were placed in between two metal, parallel plates and lubricated with dodecane to prevent drying and barreling. Each sample was preloaded to 0.005 N, which was followed by a strain sweep. Dynamic mechanical analysis was carried out at nominal compressive strain amplitudes ranging from 1% to 16% and at a frequency of 1 Hz.

Uniaxial Compression Experiments. Lubricated, uniaxial displacement-controlled compression tests were performed on cylindrical gel disks swollen at equilibrium in deionized water with an initial radius, a_0, of 4 mm and an undeformed height, h_0, of 6 mm using an Instron 5565 testing device with a 100 N load cell, as shown in Figure 1. The disks were cut from flat layers of gel and placed onto parallel plates that were fitted on the Instron. Dodecane was used as a lubricant to reduce friction and adhesion as much as possible between the plates and gel surface as well as to minimize drying of the samples.

Testing of each individual swollen sample required two steps: a calibration to determine the zero point of the strain measure, followed by a series of compressive cycles. Calibration of the gel was performed by compressing it to a maximum load of 0.3 N at a rate of 25 μm/s. Upon reaching this load, immediate unloading of the sample to 0.03 N was performed to ensure complete contact of the gel surface at the beginning of the test. Following this calibration, a single sample experienced between four and six loading−unloading cycles up to increasing maximal compressive forces at a velocity of 25 μm/s ($\dot{\varepsilon} = 4.2 \times 10^{-3}$ s^{-1}) until the gel failed. The beginning of each cycle was started at the preloaded force of 0.03 N. The resulting force, P, and the displacement data from these experiments were recorded.

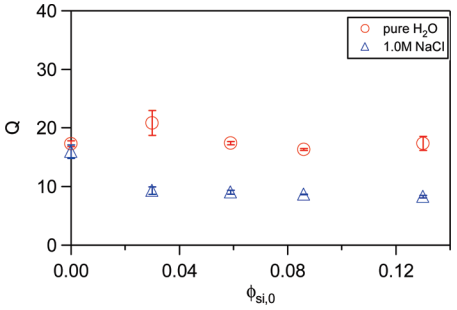

Figure 2. Swelling ratio of the hybrids Q in pure water and in 1.0 M NaCl as a function of the volume fraction of silica in the preparation conditions, $\phi_{si,0}$.

The deformation of the gel is described in terms of nominal stress, $\sigma_{nominal}$, where $\sigma_{nominal} = P/(\pi a_0^2)$, while the displacement data are expressed as an extension ratio, $\lambda = h/h_0$, where h is the deformed height.

Fracture Experiments. Single edge notch fracture experiments were performed on the gels swollen in deionized water using an Instron testing device that was fitted with custom-designed clamps to hold the sample, as shown in Figure 1. Rectangular samples (24 × 5 mm) were cut with a die from the molded flat gel layers. The thickness of each sample was individually measured and was close to 1 mm. For each sample, a cut with length C = 1 mm was made into the center edge using a sharp razor and then loaded onto an Instron 5565 tensile tester. The initial distance, H_0, defined as the distance between the edges of the two clamps, was 14 mm for each sample. Each displacement-controlled experiment was conducted at a crosshead speed of 25 μm/s until the sample fractured. Video images (Marlin, Allied Vision Technology) were taken of each sample during each experiment. The force, P, and displacement data were recorded. Slippage of the samples was prevented by using sandpaper between the grips. For these experiments, the value of nominal stress is calculated from the normalized force and cross-sectional area of the swollen sample: $\sigma_{nominal} = P/(W_0 L_0)$ where W_0 and L_0 are defined in Figure 1. The deformation is described by an extension ratio, $\lambda = H/H_0$, where H is the deformed length.

Results

Swelling Behavior. Results from the swelling experiments are shown in Figure 2. The swelling ratio, Q, in pure H_2O and 1.0 M NaCl is plotted against the volume fraction of silica, $\phi_{si,0}$, in the preparation conditions. For these experiments Q is defined as

$$Q \equiv \frac{w_{water} + w_{poly}}{w_{poly}} \quad (1)$$

where w_{water} is the total weight of water in the sample after it is swelled to equilibrium and w_{poly} is the weight of the dry polymer used to make the gel. Figure 2 shows that in pure water the presence of silica particles does not appreciably change the swelling behavior of the hydrogels. The effect of silica beads is nevertheless rather complex as opposing mechanisms arise from polymer/particle binding (increasing elasticity and deswelling) and translational entropy of surface counterions (increasing osmotic pressure and swelling). At high ionic strength (NaCl 1 mol/L) when electrostatic interactions are screened, Figure 2 clearly displays a monotonous deswelling of hydrogels with increasing amount of silica particles revealing the formation of additional physical cross-links. Qualitatively similar results have been reported for physical gels of PDMA[5] and PNIPAM[10] filled with exfoliated clay sheets.

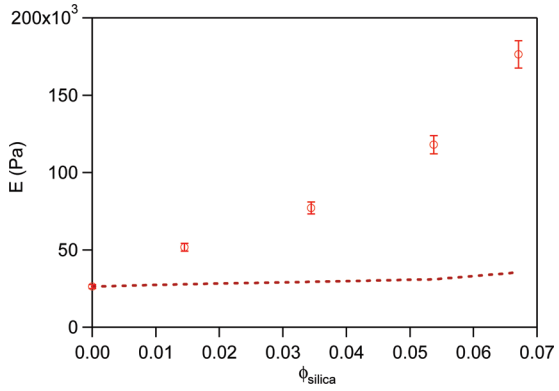

Figure 3. Modulus, E, from compression experiments versus volume fractions of silica at the testing conditions, ϕ_{silica}. The dotted line gives predicted values of the modulus calculated from the Guth−Gold model. The measured values of E are consistent with values determined from the fracture and compression experiments.

It is also interesting to notice that even at high ionic strength, all hybrid hydrogels remain perfectly transparent, while in the same conditions the silica suspension phase separates. Again, the strong adsorption of PDMA chains onto the silica surfaces introduces steric repulsions between particles and increases the stability of the hybrid network.

Modulus Measurements. Insight into the structure of PDMA−silica hydrogel hybrids can also be provided by modulus measurements. The elastic modulus, E, for each of the hybrids was determined from the linear elastic loading portion of the compression and fracture tests and is given by $E = \sigma_{nominal}/(1 - \lambda)$. An average of these values and the dynamic mechanical measurements of E were taken and plotted against the volume fraction of silica, ϕ_{si}, as depicted in Figure 3.

Figure 3 compares the experimental values of the elastic modulus to the theoretical prediction of the Guth−Gold model.[21] The Guth−Gold model provides predictions for the elastic modulus of rubbery matrix systems filled with weakly interacting filler particles. The model assumes that the filler is spherical in geometry and colloidal in nature, such that the particles develop into chains and into an eventual network at concentrations greater than 10 vol %. Based on Einstein's theory of viscosity and accounting for the mutual interactions between pairs of spheres, the Guth−Gold equation is given by[22]

$$E = E_0(1 + 2.5\phi + 14.1\phi^2) \quad (2)$$

where ϕ is the silica volume fraction and E_0 is the elastic modulus of the polymer matrix. This model is limited in that it does not account for strong interactions between particles nor does it typically account for the formation of a percolating network of interacting particles. The fact that our moduli increase by a factor of 6 even at filler concentrations as low as 5−6 vol % strongly suggests that the nanoparticles act as additional cross-link points.

Yet the swelling ratio shown in Figure 2 at high ionic strength only decreases weakly with increasing Si content, suggesting a highly inhomogeneous cross-linking in the gel and probably the existence of a percolating structure of more densely cross-linked regions.

Viscoelasticity. Dynamic mechanical experiments were performed in compression to determine the viscoelastic properties of the hybrid hydrogels at various strains. Figure 4 shows the tangent of the phase angle, δ, plotted as a function of percent strain amplitude. Since tan δ indicates the ratio between loss modulus, μ'', and the storage modulus, μ', the dynamic mechanical results show that the level of viscous dissipation is relatively high for a gel and, in the presence of silica nanoparticles, increases with the amount of silica and in cycles of greater amplitude.

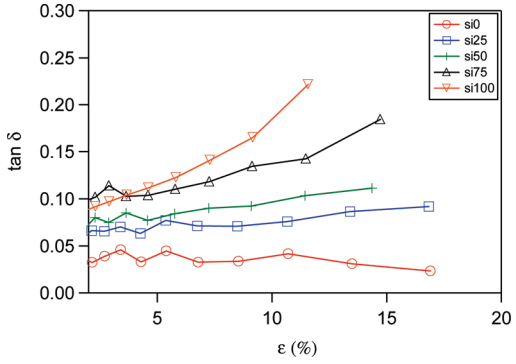

Figure 4. DMA results of the hybrid gels. tan δ is plotted as a function of percent strain. Measurements were all performed at a frequency of 1 Hz.

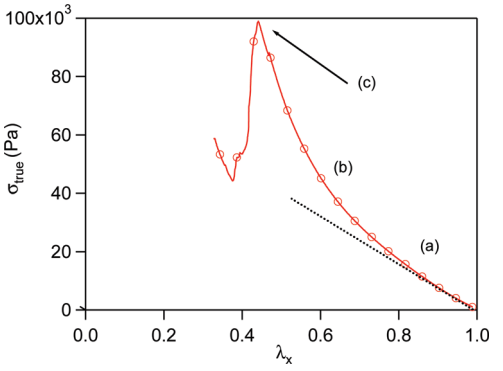

Figure 5. Typical curve of an uniaxial compression test for the hybrid materials. This curve corresponds to si50. The regions represent (a) the linear response, (b) large deformation, and (c) compressive yielding of the sample. The dashed line acts as a guide for the eye and demonstrates where linear elastic behavior of the sample is expected.

Uniaxial Compression. Although the DMA is well adapted to small strain oscillatory measurements, large strain experiments are better carried out on a mechanical testing machine. Because the samples remain relatively brittle and have a tendency to slip or break in the clamps in uniaxial tension, the large strain nonlinear elastic and viscoelastic behavior of hydrogels is more easily and reproducibly characterized in uniaxial compression (with lubricated plates).[8,23] The result of such a loading test to failure is shown in Figure 5. Region a represents the linear response of the gel, region b marks the large deformation regime of the sample where both geometric and material nonlinearities are present, and region c represents the point defined as the "compressive yielding", where the gel fails by multiple fracturing. The dashed line in this figure acts as a guide for the eye and demonstrates where linear elastic behavior of the sample is expected as well as where it begins to deviate. These measurements allow us to probe the linear elastic behavior of our samples through modulus measurements as seen in Figure 3 and their response beyond the Hookean regime and fracture in regions b and c.

In our compression experiments, the nonlinear material behavior of the hydrogels in large strains is best portrayed in the so-called Mooney representation which separates the nonlinear elastic behavior of the gel from the geometrically

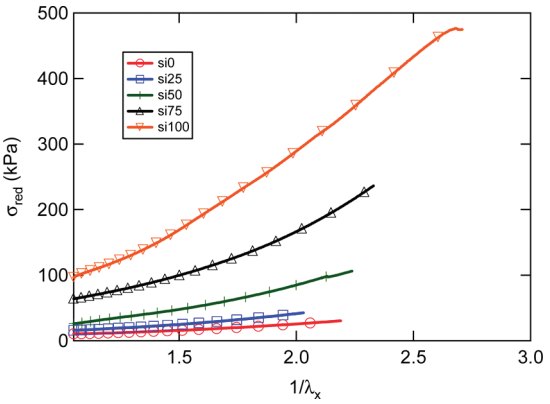

Figure 6. Reduced stress, or so-called Mooney curves, of the hybrids. Each curve is calculated from the loading cycle of a gel that undergoes fracture under compression.

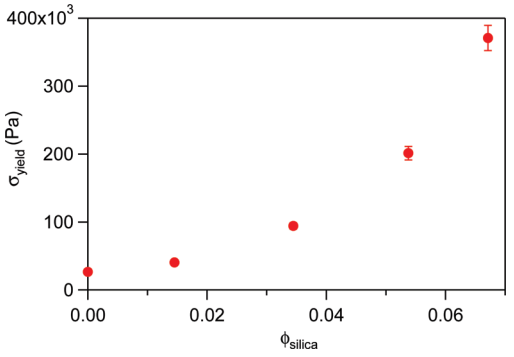

Figure 7. True stress at fracture σ_{yield} of the hybrid hydrogels as a function of ϕ_{silica} at the testing conditions. The λ values at yield are between 0.3 and 0.45.

induced one. The reduced stress, which utilizes the loading portion of the compression curves, is determined from refs 24 and 25.

$$\sigma_{red} = \frac{\sigma_{nominal}}{\lambda - 1/\lambda^2} \tag{3}$$

Figure 6 represents the reduced stress, σ_{red}, against the inverse of the extension ratio, $1/\lambda$, as it is conventionally plotted. The reduced stress physically provides a strain-dependent shear modulus μ. At low values of $1/\lambda$, the reduced stress should be equivalent to the shear modulus of the material measured in the linear portion of the curve. If the reduced stress remains constant as a function of λ, classical rubber elasticity behavior is recovered. This behavior is nearly the case for the pure PDMA sample which only shows a very moderate strain hardening at higher strains. However, strain hardening becomes more pronounced as the filler concentration increases. The underlying molecular reason behind that strain hardening in polymer networks is the transition from an entropic elasticity of the chain to an enthalpic elasticity when the chain is fully stretched. In well-cross-linked and homogeneous networks, this strain hardening is very sharp. As the filler concentration increases, we observe very progressive strain hardening starting at lower and lower strains. This feature is indicative of a wide distribution of finite chain extensibilities and hence of elastic strand molecular weights within the hybrid networks.

When the compressive deformation on the gel becomes large enough to fracture it, it is worthwhile to examine the ultimate failure resistance. The difference between the pure

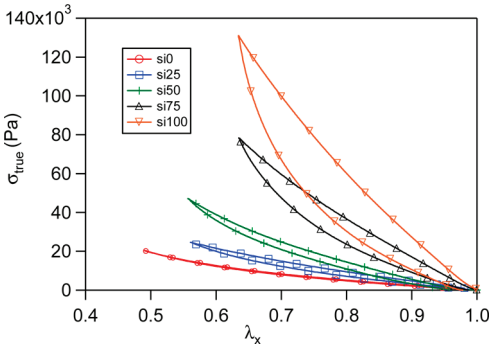

Figure 8. Representative loading unloading curves of the hybrids in compression. Note the lack of hysteresis in the pure PDMA sample in comparison to the hybrids with silica.

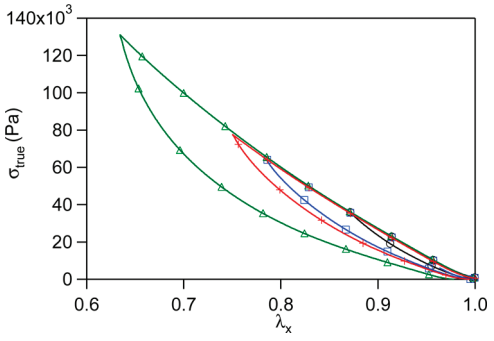

Figure 9. Loading/unloading curves of si100 under compression. Loading and unloading cycles are performed in immediate succession with the same sample at increasing levels of maximum strain.

conventional network when compared to the filled hydrogel hybrids can be seen in Figure 7, which demonstrates a strengthening behavior of the hybrids in addition to a stiffening. In this figure, the true stress at yielding is plotted as a function of volume fraction of silica, ϕ_{si}, and increases very significantly with it. These figures can be interpreted to describe the structure of the PDMA−silica hybrids as it relates to the behavior observed.

While the loading to failure tests from Figure 5 provide insight into the behavior of the hydrogels, one very revealing feature of these materials is the hysteresis that exists after they are unloaded at large deformations. This behavior can be a signature of the nature and characteristic time of molecular events causing a reorganization of the structure in the gel and can explain its instantaneous stiffness. When compared to the typical stress−strain curves of the unmodified PDMA gel, the hydrogel hybrids are markedly different in behavior. The effect of silica on the properties of the gels beyond the linear elastic regime can be seen in Figure 8. The behavior of the pure PDMA sample over a large range of strains is given as a guide for the eye. As expected from a conventional chemical gel, no hysteresis appears in the pure PDMA network. On the contrary, the loading−unloading portions of the hybrids deviate from one another during the same experiment, exhibiting a form of dissipation.

Such results require us to check whether the hysteresis loops cause permanent damage over the time scale of the repeat loading/unloading experiments and whether the amplitude of the hysteresis is dependent on the maximum strain reached during the loading stage. One example of consecutive cycles on the same sample at decreasing values of λ_{min} is shown in Figure 9. From this graph, it is clear that all the loading curves fall on the same master curve, implying that

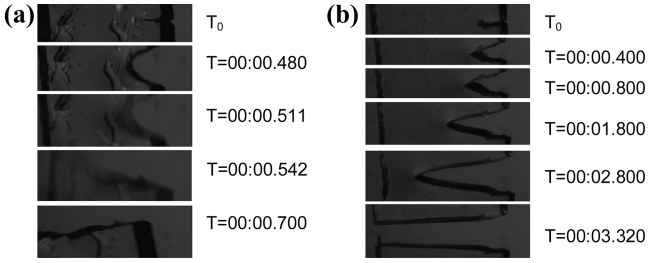

Figure 10. Time lapsed images of SEN tests for hybrids of (a) si0 and (b) si100. The indicated times are given in mm:ss. T_0 represents the sample prior to crack propagation.

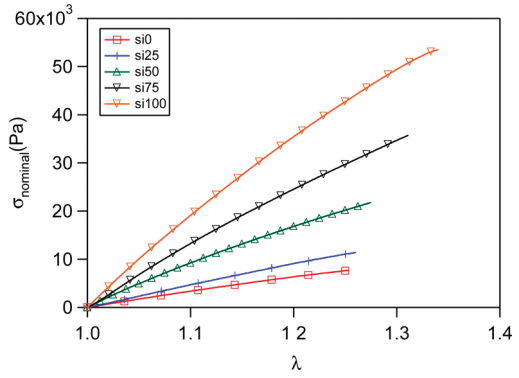

Figure 11. Typical stress−strain curves up to the point where the crack has fully propagated through for each sample. Results for the hybrid gels with varying amounts of silica from SEN experiments.

the structure of the gel returns to its initial state after each deformation cycle. However, the energy dissipated during the cycle depends markedly on the maximum strain achieved (in compression on the value of λ_{min}). This behavior shows a complete absence of Mullins effect, i.e., a permanent or at least very slowly relaxing change in structure after the first cycle. This behavior is in contrast with observations for the double-network gels.[15]

Fracture Tests. Although the results from the compressive experiments are indicative of the mechanical strength of a material, they do not represent a true test of fracture toughness. To determine this property, tests need to be carried out in tension and with a notched sample. As described above, we performed single-edge notch fracture tests on our hydrogels to determine their fracture toughness in severe conditions of stress localization. Parts a and b of Figure 10 capture time lapsed video images of the SEN tests for si0 and si100, respectively. The frame by frame images show that crack propagation slows down markedly with the addition of silica.

A more quantitative analysis of the fracture tests is shown in Figure 11, which graphs the nominal stress, σ_{nom}, versus the extension ratio, λ, of a typical SEN fracture curve for each sample. The nominal stress is defined here as the measured force normalized by the initial cross-sectional area of an unnotched part of the sample, and the extension ratio λ is the deformed length of the sample normalized by its initial length. From these curves, a critical energy release rate in mode I can be determined using the analysis of Rivlin and Thomas.[26,27] On the basis of an energy balance, it can be determined that crack propagation occurs when the energy release rate, G, is greater than that of the critical value of G_c:

$$G = \frac{1}{W_0}\left(\frac{\partial U}{\partial c}\right)_\lambda = 2K(\lambda)cU_0(\lambda) \qquad (4)$$

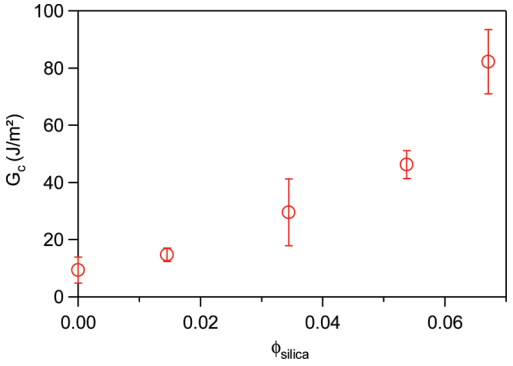

Figure 12. Energy release rate, G_c, determined from SEN tests versus the volume fraction of the silica in the testing conditions.

where

$$U_0(\lambda) = \mu\left(\lambda^2 - \left(\frac{2}{\lambda}\right) - 3\right) \qquad (5)$$

and $K(\lambda) = 3/\sqrt{\lambda}$ is a constant which depends on the geometry and the stretching ratio, c is the length of the cut, W_0 is the thickness of the gel, $U_0(\lambda)$ is the strain energy density of the gel at a given extension ratio λ, and μ is the shear modulus. The critical G_c values for the hybrids at the threshold for crack propagation are plotted in Figure 12 by applying eqs 4 and 5 to Figure 11. The λ values are the maximum extension ratios in Figure 11. As seen in the graph, the addition of silica increases significantly the critical energy release rate G_c for crack propagation. Although this geometry does not easily permit a measurement of crack velocity in steady state, the marked slowdown observed in the videos suggests that we are underestimating the toughness of the highly filled systems. These results unambiguously show that the silica nanoparticles toughen and stiffen the gel.

Discussion

Structure and Small Strain Behavior. Based on the combination of experiments carried out, a self-consistent picture emerges of the structure of the hybrid hydrogels. The fact that the silica nanoparticles do not escape during the swelling to equilibrium points toward an adsorption process of the polymer on the surface of the silica.

Can we be more quantitative about the adsorption process? From previous experiments performed by Petit et al.[19] with Ludox nanoparticles from the same manufacturer, it was shown that polymer chains of PNIPAM and PDMA were both strongly interacting and adsorbing onto silica surfaces. The adsorption isotherms were almost the same for the two polymers, and the maximum amounts of adsorbed polymers were $\Gamma_{max} \cong 1$ mg/m^2. Moreover, from calorimetric experiments performed on PNIPAM/silica mixtures, it was shown that at low coverage ($\Gamma < 0.5$ mg/m^2) the polymer chains strongly adsorbed in a flat conformation on the surface of the nanoparticles, although at higher coverage ($0.5 < \Gamma \leq 1$ mg/m^2) mainly loops and tails were formed in the outer shell with swelling and responsive properties.

Using Ludox SM-30 nanoparticles with an average specific surface $S_{sep} = 140$ m^2/g, the maximum polymer adsorption ($\Gamma_{max} = 1$ mg/m^2) expected is for a silica to polymer weight ratio 7 to 1. In the case of the hydrogel si100 with a silica to polymer weight ratio of 3, we can estimate that a maximum of about 40% of the total amount of PDMA material is adsorbed onto the silica surface, while the remaining

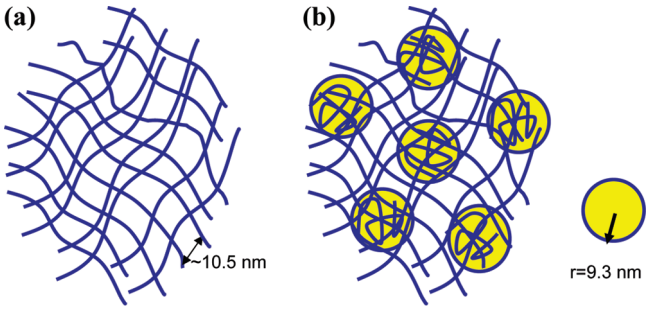

Figure 13. Schematic of (a) a pure PDMA gel and (b) silica-filled PDMA gels. (a) In pure PDMA, chemical cross-links are formed from MBA. (b) In silica-filled PDMA gels, adsorption of the polymer onto the silica creates a physical network in the PDMA chemical network.

60% form the polymer matrix in the interparticle domain. Consequently, if we assume that PDMA chains are adsorbed onto the silica nanoparticles during the initial step of the polymerization, we can draw a schematic picture of the hybrid network (see Figure 13) with (1) silica nanoparticles, with a mean diameter of about 20 nm, randomly distributed in the polymer network; (2) a dense polymer shell of adsorbed PDMA with a thickness of about 1−2 nm depending on the swollen state of the layer; and (3) a PDMA network in the bulk which should have a structure similar, or perhaps a little bit less cross-linked, compared to the one obtained without inorganic particles (Figure 13a).

To this picture, the contribution of counterions coming from the self-dissociation of silanol groups at pH close to 7 needs to be taken into account. These counterions, which are embedded into the network, contribute positively to the osmotic pressure and provide additional swelling at equilibrium in pure water. On the other hand, the formation of additional cross-links (physical ones) between PDMA and silica are expected to decrease the swelling value at equilibrium. The equilibrium swelling data given in Table 1 and pictured in Figure 2 indicate that these two opposite effects offset each other in pure water and that in these conditions the swelling appears to be independent of the amount of added silica. At high ionic strength, the electrostatic contribution vanishes and all hydrogels behave as neutral networks. This is typically observed for all hybrid networks which show a 50% deswelling in salt compared to pure water, whereas the swelling behavior of the neutral, pure PDMA gel (si0) remains practically independent of the presence of salt.

Further analysis can be carried out with the small strain behavior of the hybrids which reflects the structure. From Figure 3, the nanoparticles in the gel strongly stiffen the PDMA network. A comparison of the measured Young's moduli with the predictions of the Guth−Gold model shows that the experimental values are much greater than the theoretical ones for a weakly interacting filler in a continuous matrix. Instead of behaving like a dilute filler, the silica filler plays a similar role as the clay in PNIPAM−clay gels[28] and PDMA−clay gels,[5] where the modulus of the gels increases significantly with clay concentration. The clay platelets in these polyacrylamide systems provide additional multifunctional cross-linking points to the network and hence increase the density of elastically active chains. Our results provide evidence that the silica in the PDMA act similarly as additional physical cross-links in the network, and this behavior can only happen if the polymer strands are strongly adsorbed onto the nanoparticles.

From the modulus measurements of the pure network, the theoretical molecular weight between chemical cross-links, M_c, of the unfilled PDMA gel can be determined. If the chains in the network are considered ideal polymer strands that are attached to nonfluctuating cross-links, the PDMA can be modeled as an affine network.[29,30] Obtaining the Young's modulus from the results in Figure 3, M_c, for the unmodified, swelled PDMA gel is determined from the theories of rubber elasticity[29,30] and swelling:[31,32]

$$\mu = \frac{E}{3} = \nu_c kT \frac{\langle R^2 \rangle}{\langle R_0^2 \rangle} = \frac{\rho \phi_{DMA} RT}{M_c} \left(\frac{Q}{Q_0} \right)^{2/3} \qquad (6)$$

where μ is the shear modulus, R is the universal gas constant, $T = 298$ K, k is Boltzman's constant, ν_c is the number of network strands between chemical cross-links per unit volume, ρ is the polymer density in the dry network, and ϕ_{DMA} is the polymer volume fraction in the gel at the testing conditions. Q and Q_0 are the swelling ratios at the testing and preparation conditions, respectively, and the last term in eq 6 is the corrective term due to the prestretching of the chains during the swelling process. Using the above values, an approximate value of M_c for PDMA is calculated to be ~42 000 g/mol.

It is interesting to compare the additional density of cross-link points provided theoretically by the nanoparticles with the actual increase in modulus. If each silica nanoparticle is well separated from its neighbor and we have an average radius r of 9.3 nm, the number density of nanoparticles is given by

$$\nu_{particles} = \frac{3\phi}{4\pi r^3} = \phi \times 3 \times 10^{23}\ m^{-3} \qquad (7)$$

The number density of elastic strands due to chemical cross-links can be directly obtained from the modulus of the unfilled PDMA and eq 6. This value is determined to be $n = 1.35 \times 10^{24}\ m^{-3}$. Therefore, the ratio of particles/chemical cross-link varies between 0.003 and 0.015, while the additional density of elastically active chains (from the modulus measurement) increases 7-fold. This gives an idea of the multifunctionality of the nanoparticle which would create between 3 and 500 new elastic chains per particle.

Large Strain Behavior. While the mechanical experiments at small strains probe the structure and the molecular organization of the gel, a better understanding of the strength of the silica−network interaction can only be obtained at large strains. The presence and reproducibility of the hysteresis loops under large compressive strains (Figures 8 and 9), as well as the observed lack of a well-defined strain level where strain hardening sets in (Figure 6), provide insight into the nature of the particle/chain interactions inside the gel.

One explanation for the presence of hysteresis loops in the hybrids can be attributed to the deadsorption and readsorption of the PDMA chains during the time scale of each compression cycle. Similar hysteresis loops have been observed in double network gels,[15] hydrophobically modified polyelectrolyte gels,[33] and triblock copolymer gels.[4] The results from these experiments generally indicate a disruption in the structure of the hybrid network under compression. It is important to keep in mind that from the point of view of deformation uniaxial compression is identical to equibiaxial tension for an incompressible material.

Support for this desorption/readsorption mechanism in our hybrid systems can be seen in Figure 9 in which the typical loading curves for sample si100 is repeatable over a series of cycles. These observations suggest that there is no bond breakage or permanent damage apparent in the gel network after each cyclic load, since full recovery of the

initial stiffness of the gel exists during the time scale of the experiment. Because no trace of permanent damage is apparent for continuous repeated loading and unloading, the recovery of the strength in the material is attributed to the noncovalent interactions between the PDMA chains and the silica nanoparticles.

These properties contrast what has been proposed in other polymer-based systems. In double network gels, for example, significant hysteresis has been noted in their first loading cycle. However, permanent damage after this cycle leads to a large decrease in stiffness in subsequent loadings.[15] Similarly, significant hysteresis has been noted in uniaxial compression experiments of polyelectrolyte hydrogels, where strain-induced ionic clustering of charged chains results in this behavior.[4] Although this kind of interaction between silica nanoparticles and the PDMA network does exist, energy dissipation in the PDMA hybrids is not caused by this mechanism, since the silica nanoparticles are weakly charged and the gels are neutral. Clusters of short hydrophobic chains in charged gels have produced very large additional hysteresis during the loading cycles in compression.[8] This large hysteresis has not led however to an increase in toughness, implying that the presence of hysteresis alone is not enough to result in high toughness.

The proposed mechanisms that explain the behavior of the PDMA hydrogel hybrids can be compared to the properties of both elastomers and block copolymer gels.[5] Although semipermanent damage, known as the Mullins effect, is commonly seen in carbon black rubbers that have spherical filler nanoparticles, the recovery of virgin strength in elastomers has been noted generally after a long time and at higher temperatures but at times after 30 min.[34] The interactions between particles and polymers in such elastomers are mostly not permanent in nature. This property in filled elastomers can be used to describe the behavior of PDMA hybrids in Figures 8 and 9 and explains the dynamic mechanical data in Figure 4, where viscoelasticity increases with particle concentration and strain amplitude (an effect called Payne effect[35]). The viscoelastic behavior of our hybrids can be explained by the presence of dissipative mechanisms at the molecular level and are consistent with the picture of weak cross-linking points brought forward.

The silica−polymer interaction in our systems can also be qualitatively compared to the behavior of nonchemically cross-linked PNIPAM gels filled with hectorite,[11] where the ability to recover from some of the compression loads was also observed. However, these PNIPAM gels recover only half their original length after loading and have been described as similar in mechanical behavior as rubbers with a very low cross-link density which show plasticity. The recovery of these gels has been attributed to the high mobility of the polymer chains in the solvent and to the narrow molecular weight distribution between cross-links. Because our PDMA gels are chemically and physically cross-linked, long-distance mobility of the polymer chains is unlikely. Evidence of a wide rather than narrow molecular weight distribution between cross-links is seen in the Mooney plots in Figure 6. Full recovery of the shape of the gel and of its initial modulus implies that the cross-linked structure remains intact precluding any large scale flow within the material.

When our system is compared with chemically cross-linked PNIPAM gels with clay sheets, a better understanding of the relationship between silica and the network emerges. For a chemically cross-linked gel with clay sheets, the distribution of molecular weight between cross-links in the system is dependent on the amount of MBA per inorganic particle. When the ratio of clay particles/MBA is much greater than one in these systems, the PNIPAM chains are lightly chemically cross-linked and form an inhomogeneous network.[36] These networks result from the affinity of the MBA for the broadly dispersed clay and do not have a uniform spatial distribution of chemical cross-link points throughout the gel. On the other hand, a high value of MBA per clay particle leads to gels that undergo brittle fracture, since the distribution of the average molecular weight between cross-links is more homogeneous throughout the network.[36] In both cases, the addition of reinforcing agents leads to larger values of toughness. Although Haraguchi et al. stress the multifunctionality of the physical cross-links,[2] we would like to emphasize the wide distribution of finite extensibilities of network chains that the physical cross-links contribute. In essence, the desorption of a polymer chain from a silica nanoparticle when it reaches its maximum extensibility occurs at a range of macroscopic strains and leads to a progressive strain hardening.

Compressive Yield and Fracture. The incorporation of the silica nanoparticles in the gels has a notable effect on their compressive yield strengths and fracture toughnesses. As seen from our experiments, the amount of energy required for failure increases under compression and tension when greater amounts of silica are incorporated in the PDMA network.

Under compression, the trend for the PDMA−silica hybrids in Figure 7 has been documented in physically cross-linked PDMA−clay and PNIPAM−clay systems.[36] In these gels, the addition of nanoparticles increases the compressive yield point due to the additional physical cross-linking points.[36] This contribution of strength from the silica to the PDMA network is also apparent in our experiments and is consistent with the absorption and dissipative mechanism in our hybrids.

The slowdown of crack propagation, as seen in the images of the SEN tests, provides further evidence of the silica−polymer interactions. While the amount of elastic energy provided to the system actually increases, the crack propagation rate decreases. This behavior strongly supports the presence of a much more effective dissipative mechanism at the crack tip. Such mechanisms are able to average the stresses and absorb the strain energy in a nonlocalized way. The silica stiffens the gel network by creating additional physical cross-linking points, but the breakable nature of the bonds and a broad distribution of distances between cross-links creates most likely a wide dissipative zone ahead of the crack tip as described by Gong et al. for double network gels.[18] On a more molecular level, one can speculate that the dissipation occurs as a result of the breakage of the inter actions between the polymer chains in the network and the silica nanoparticles. This behavior is likely to occur as the material is highly strained near the crack tip.

Comparison to the Lake−Thomas Theory and Threshold Fracture. The fracture toughness results, as seen in Figures 11 and 12, are surprising when compared to theoretical predictions of general rubber network fracture behavor. Although an increasing modulus is noted in Figure 3, the gels maintain the same extensibility at fracture and therefore toughen. As shown in Figure 11, fracture of the hybrids occurs at extension ratios between 1.25 and 1.35. This result suggests that the macroscopic extensibility at fracture is mainly controlled by the average extent of chemical cross-linking while the filler contributes more densely cross-linked regions and heterogeneity. An energy dissipation argument would however point to the existence of a dissipative mechanism slowing crack propagation.

This result challenges qualitatively the Lake−Thomas theory,[7] which predicts that a decrease in strain at fracture for nondissipative elastomers—which includes rubbers at high temperature and low strain rates as well as our gels—leads to an increase in modulus. The Lake−Thomas theory proposed that the threshold fracture of an elastic network was related to the energy necessary to stretch to fracture each elastic strand crossing the plane of fracture, G_{LT}. This hypothesis leads then to the relation[7]

$$G_{LT} \cong \frac{\rho a}{2M_0} \sqrt{N_c} U_{mol} \quad (8)$$

where N_c is the average number of monomers per elastic strand, ρ is the density of the polymer in the gel, M_0 is the monomer molar mass with a length a, and U_{mol} is the energy required to rupture a C−C covalent bond.

Qualitatively the Lake−Thomas theory predicts that the gels will become more brittle as the density of elastic strands increases and their average length N_c decreases. Figure 11 shows the contrary. The interactions between the silica nanonanoparticles and the polymer provide a form of weaker and breakable physical cross-links which will likely break at a range of values of local stress due to the distribution in finite extensibilities of the chains. These weaker bonds in a strong chemical network create significant dissipation not only directly at the crack tip as the Lake−Thomas theory implies, but certainly in a significant volume ahead of the crack tip because of the stress concentration ahead of the crack. Whether these dissipative mechanisms would vanish at very low crack speed remains an open question for the time being.

It is also interesting to make some quanitative comparisons in the case of pure PDMA. Based on eq 7, a predicted G_{LT} for the pure, unfilled PDMA gels gives an energy release rate of 0.48 J/m^2. This theoretical value is much lower than those found experimentally and can be explained by the presence of some dissipative defects such as pendant chains in the pure PDMA gel. Fracture experiments at lower strain rates should be carried out to investigate how far from threshold fracture are the gels.

Conclusions

Novel PDMA hydrogel hybrids were successfully synthesized and characterized. These gels consisted of various concentrations of colloidal silica nanoparticles. Our experiments and observations point clearly to a nanocomposite picture from a structural and mechanical point of view. As seen in Figure 13, a pure chemically cross-linked gel of PDMA (Figure 13a) is compared to the proposed hydrogel hybrid model (Figure 13b). Evidence from our experiments suggests that the silica is strongly adsorbed and creates a much wider distribution of molecular weight between physical cross-links within the more homogeneously chemically cross-linked gel.

From a mechanical perspective, these hydrogels significantly toughen and stiffen with increasing amounts of inorganic nanoparticles. This behavior is qualitatively different from other types of tough gels. Although their fracture behavior contradicts the predictions of the Lake−Thomas theory for unfilled rubbers, they do not exhibit a Mullins effect, the signature of the breakup of a filler network that occurs in filled elastomers. Moreover, their mechanical behavior is more similar to that of the well-characterized physically cross-linked inorganic−organic systems of Haraguchi[2,6,28] than to that of conventional chemically cross-linked gels, even though the small-strain modulus and the total number of elastically active chains increases. Considering that these gels could be viewed as a form of double network gel, their mechanical properties also cannot compare to the double network gels formed by Gong et al.[13,15] where the fracture of covalent chemical bonds is important.

Such inconsistencies were explained in terms of the nature of particle−chain interactions and the corresponding structure of the gel. On the basis of our experiments, we propose that the silica nanoparticles act like weak physical cross-links within a strong chemical network. The addition of silica likely disturbs the homogeneity of the network, increasing the number of particles in the system and broadening the distribution of elastic chain lengths within the gel. This depiction of the silica within the PDMA gels, reinforced by the near lack of change in the swelling ratio with increasing organic filler concentration, explains the toughness and fracture behavior of the gels, along with the repeatability of the compression experiments. Lastly, the PDMA−silica system challenges the notion that silica nanoparticles could not be used as reinforcing agents in organic−inorganic structures. Based on this work, there is evidence that silica could be independently used to physically cross-link a gel.

These gels are therefore good model systems that provide insight into the interactions of inorganic particles in chemically cross-linked gels; however, questions still remain about the large strain behavior in these gels. One future area of research to pursue would be to understand the physical and molecular origin of the hysteresis under compression for the hybrids. Further experimentation is also required to understand how the nanoparticles are organized at very high strains and the properties at the crack tip during fracture.

Acknowledgment. The authors acknowledge Linn Carlsson and Tetsuhara Narita for dynamic light scattering measurements of the silica nanoparticles. This project was financially supported by the French ANR Blanc programme: project AdhGel.

References and Notes

(1) Tanaka, Y.; Gong, J. P.; Osada, Y. *Prog. Polym. Sci.* **2005**, *30*, 1–9.
(2) Haraguchi, K. *Macromol. Symp.* **2007**, *256*, 120−130 210.
(3) Baumberger, T.; Caroli, C.; Martina, D. *Eur. Phys. J. E* **2006**, *21*, 81–89.
(4) Seitz, M. E.; Martina, D.; Baumberger, T.; Krishnan, V. R.; Hui, C. Y.; Shull, K. R. *Soft Matter* **2009**, *5*, 447–456.
(5) Haraguchi, K.; Farnworth, R.; Ohbayashi, A.; Takehisa, T. *Macromolecules* **2003**, *36*, 5732–5741.
(6) Haraguchi, K. *Curr. Opin. Solid State Mater. Sci.* **2007**, *11*, 47–54.
(7) Lake, G. J.; Thomas, A. G. *Proc. R. Soc. London* **1967**, *300*, 108−119.
(8) Miquelard-Garnier, G.; Hourdet, D.; Creton, C. *Polymer* **2009**, *50*, 481–490.
(9) Huang, T.; Xu, H. G.; Jiao, K. X.; Zhu, L. P.; Brown, H. R.; Wang, H. L. *Adv. Mater.* **2007**, *19*, 1622–+.
(10) Haraguchi, K.; Takehisa, T.; Fan, S. *Macromolecules* **2002**, *35*, 10162–10171.
(11) Liu, Y.; Zhu, M.; Liu, X.; Zhang, W.; Sun, B.; Chen, Y.; Adler, H.-J. P. *Polymer* **2006**, *47*, 1–5.
(12) Haraguchi, K.; Li, H.-J.; Matsuda, K.; Takehisa, T.; Elliott, E. *Macromolecules* **2005**, *38*, 3482–3490.
(13) Gong, J. P.; K., Y.; Kurokawa, T.; Osada, Y. *Adv. Mater.* **2003**, *15*, 1155–1158.
(14) Tanaka, Y.; Kuwabara, R.; Na, Y.-H.; Kurokawa, T.; Gong, J. P.; Osada, Y. *J. Phys. Chem. B* **2005**, *109*, 11559–11562.
(15) Webber, R. E.; Creton, C.; Brown, H. R.; Gong, J. P. *Macromolecules* **2007**, *40*, 2919–2927.
(16) Brown, H. R. *Macromolecules* **2007**, *40*, 3815–3818.
(17) Tanaka, Y. *Europhys. Lett.* **2007**, *78*, 56005–56010.
(18) Yu, Q. M.; Tanaka, Y.; Furukawa, H.; Kurokawa, T.; Gong, J. P. *Macromolecules* **2009**, *42*, 3852–3855.
(19) Petit, L.; Bouteiller, L.; Brulet, A.; Lafuma, F.; Hourdet, D. *Langmuir* **2007**, *23*, 147–158.
(20) Heinrich, G.; Kluppel, M. *Adv. Polym. Sci.* **2002**, *160*, 1–44.
(21) Guth, E.; Gold, O. *Phys. Rev.* **1938**, *53*, 322.
(22) Guth, E. *J. Appl. Phys.* **1945**, *16*, 20–25.

(23) Miquelard-Garnier, G.; Creton, C.; Hourdet, D. *Soft Matter* **2008**, *4*, 1011–1023.
(24) Rivlin, R. S.; Saunders, D. W. *Philos. Trans. R. Soc. London, Ser. A* **1951**, *243*, 251–288.
(25) Mooney, M. *J. Appl. Phys.* **1940**, *11*, 582–592.
(26) Rivlin, R. S.; Thomas, A. G. *J. Polym. Sci.* **1953**, *10*, 291.
(27) Greensmith, H. W. *J. Appl. Polym. Sci.* **1963**, *7*, 993–1002.
(28) Haraguchi, K.; Li, H.-J. *Macromolecules* **2006**, *39*, 1898–1905.
(29) James, H. M.; Guth, E. *J. Chem. Phys.* **1947**, *15*, 669–683.
(30) James, H. M. *J. Chem. Phys.* **1947**, *15*, 651–668.
(31) Flory, P. J. *J. Chem. Phys.* **1950**, *18*, 108–111.
(32) Flory, P. J. *J. Chem. Phys.* **1977**, *66*, 5720–5729.
(33) Miquelard-Garnier, G.; Creton, C.; Hourdet, D. *Macromol. Symp.* **2007**, *256*, 189−194, 210.
(34) Heinrich, G.; Kluppel, M.; Vilgis, T. A. *Curr. Opin. Solid State Mater. Sci.* **2002**, *6*, 195–203.
(35) Payne, A. R.; Whittaker, R. E. *J. Appl. Polym. Sci.* **1971**, *15*, 1941–&.
(36) Haraguchi, K.; Song, L. *Macromolecules* **2007**, *40*, 5526–5536.
(37) Brandrup, J., Immergut, E. H., Eds.; *Polymer Handbook*, 3rd ed.; John Wiley and Sons: New York, 1989.